# AN INVESTIGATION OF PLASTIC TORSION IN CIRCULAR PRISMATIC BARS WITH A CONCENTRIC OR ECCENTRIC HOLE USING THE SAND-HEAP ANALOGY

A Thesis

by

GERALD JOHN CAREY, JR.



Submitted to the Graduate School of the
Agricultural and Mechanical College of Texas in
partial fulfillment of the requirements for the degree of

MASTER OF SCIENCE

May 1963

Major Subject: Aerospace Engineering

(4) NA
(5) 8617500

# (6) AN INVESTIGATION OF PLASTIC TORSION IN CIRCULAR PRISMATIC BARS WITH A CONCENTRIC OR ECCENTRIC HOLE USING THE SAND-HEAP ANALOGY

(7) NA
(8) NA
(9) NA

(12) 45p
(13) NA
(14) NA
(15) NA
(16) NA
(17) NA
(18) NA
(19) NA
(20) ill.
(21) Master's thesis

A Thesis

(10) by

GERALD JOHN CAREY, JR.

Submitted to the Graduate School of the
Agricultural and Mechanical College of Texas in
partial fulfillment of the requirements for the degree of

MASTER OF SCIENCE

(11) May 1963

Major Subject: Aerospace Engineering

In C.

# AN INVESTIGATION OF PLASTIC TORSION IN CIRCULAR PRISMATIC BARS WITH A CONCENTRIC OR ECCENTRIC HOLE USING THE SAND-HEAP ANALOGY

A Thesis

by

GERALD JOHN CAREY, JR.

Approved as to style and content by:

_____
(Chairman of Committee)

_____
(Head of Department)

May 1963

## ACKNOWLEDGMENTS

I wish to express my sincere thanks to Doctor Charles H. Samson, Jr. and Professor Harry J. Sweet for their help, interest, and many valuable suggestions during this investigation.

My particular gratitude is given to Mr. Ted J. Meiller for his assistance and suggestions in the construction of the test specimens.

To my wife, Joan, who has been of invaluable assistance, I express my sincere appreciation.

TABLE OF CONTENTS

## LIST OF FIGURES

## LIST OF TABLES

## LIST OF PLATES

## LIST OF SYMBOLS

| | |
|---|---|
| $x, y, z$ | Rectangular coordinates |
| $\tau_{xy}, \tau_{xz}, \tau_{yz}$ | Shearing-stress components |
| $\gamma_{xy}, \gamma_{xz}, \gamma_{yz}$ | Shearing-strain components |
| $\epsilon_x, \epsilon_y, \epsilon_z$ | Unit elongation in x-, y-, and z- directions |
| $\sigma_x, \sigma_y, \sigma_z$ | Normal components of stress parallel to x-, y-, and z- directions |
| $u, v, w$ | Components of displacements |
| $\theta$ | Angle of twist per unit length |
| $\phi$ | Warping function |
| $b$ | Number of basic dimensions |
| $c$ | Offset distance from center of bar to center of hole |
| $F$ | Elastic stress function |
| $F_1$ | Plastic stress function |
| $G$ | Modulus of elasticity in shear |
| $h$ | Height of cylinder in sand-heap |
| $I_2$ | Second invariant of the stress tensor |
| $k$ | Yield shearing stress |
| $m$ | Maximum slope of sand-heap |
| $n$ | Number of dimensional quantities |
| $p$ | Pressure acting on membrane |
| $R$ | Radius of circular bar |
| $r$ | Radius of circular hole |
| $S$ | Area of hole |

| | |
|---|---|
| $s$ | Surface tension developed in membrane |
| $s_1$ | Number of non-dimensional $\pi$ terms |
| $V$ | Total volume |
| $V_o$ | Volume of sand on tray |
| $T$ | Torque |
| $z$ | Vertical deflection of membrane |

# CHAPTER I

## INTRODUCTION

In determining the shear stresses developed in a circular shaft by the action of a twisting moment, the strength of materials approach provides an exact solution. One major assumption in this analysis is that plane sections normal to the axis before twisting remain so after twisting.

This assumption is not valid for a non-circular prismatic bar or any cross section with a non-concentric circular hole. The solution to this problem is more difficult and considered in the theory of elasticity. As will be shown, the theory of elasticity embodies a solution assuming a linearly elastic material and involving the introduction of a stress function, the appropriate derivatives of which define the shearing stresses. If the particular stress function satisfies the conditions of equilibrium, boundary conditions, and compatibility, the solution is mathematically unique.

As the torque is increased, material will pass from the elastic to the plastic state. There is a limit to the ability of the cross section to withstand increasing torque. This limit is called the plastic strength in torsion; it represents that value of torque above which there is no resistance to flow and complete failure results with continued deformation. At this condition torque is no longer a function of rotation.

The purpose of this research was to investigate and predict the plastic strength in torsion of circular prismatic bars with a concentric or eccentric hole.

# CHAPTER II

## THEORY OF TORSION ANALOGIES

### The Membrane Analogy for Elastic Torsion

Consider a cylindrical or prismatic bar of constant cross section which is twisted and held in equilibrium by twisting moments applied at its ends. The cross section of such a bar is shown in Figure 1. The bar is considered to be composed of an isotropic material possessing the idealized stress-strain relationship for an elastic, perfectly plastic material shown in Figure 2.

Increasing torque causes the material to pass from the elastic region (line AB, Figure 2) into the perfectly plastic range (line BC, Figure 2). After a point in the cross section reaches the yield stress in shear (point B), this maximum shearing stress remains a constant value k as increasing torque causes an increase in the plastic region of the bar. Before examining the plastic behavior of the prismatic cross section, consider the stress characteristics in the elastic range.

The exact solution to the problem of elastic torsion of prismatic bars was first postulated by Saint-Venant in 1855.[1*] The displacements in the x and y directions due to rotation of the cross sections are designated by u and v, respectively. The warping of the cross section is denoted by w and defined by the function $\phi$. These displacements are assumed to be:[2]

* References cited are listed numerically at the end of this thesis.

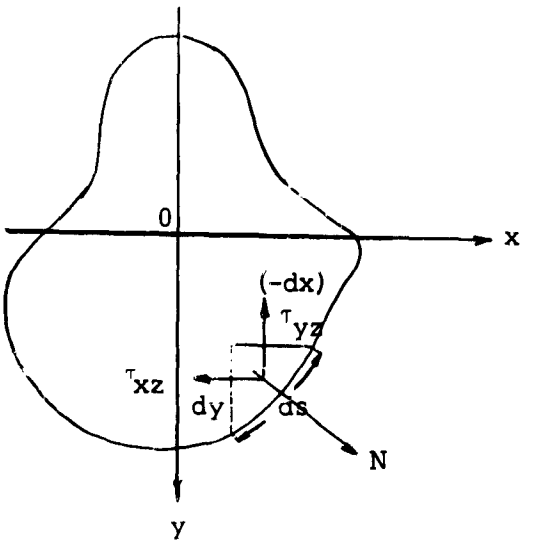


Figure 1. Two-Dimensional View, Prismatic Cross Section Subjected to Torsion.

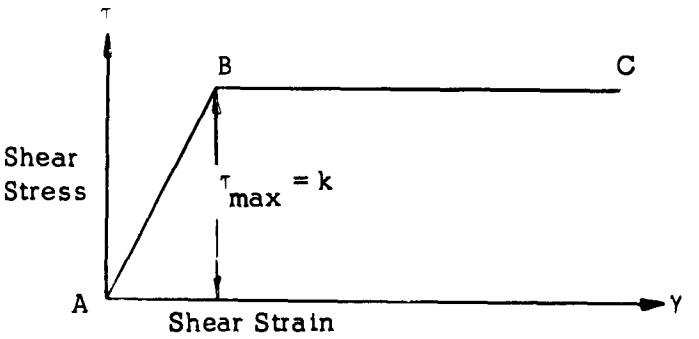


Figure 2. Idealized Shearing Stress-Strain Curve

$$u = -\theta zy$$

$$v = \theta zx$$

$$w = \theta \phi(x,y) \tag{1}$$

With reference to Figure 3, $\theta z$ is the angle of rotation of the cross section at a distance z from the origin 0.

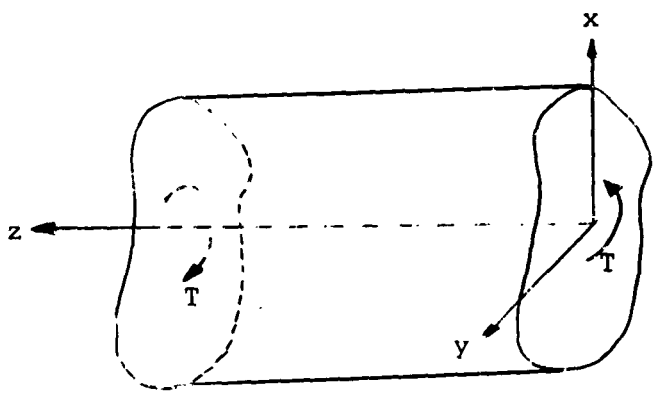


Figure 3. Three-Dimensional View, Prismatic Cross Section Subjected to Torsion

In terms of the assumed displacements u, v, and w, the components of strain are[3]

$$\epsilon_x = \epsilon_y = \epsilon_z = \gamma_{xy} = 0$$

$$\gamma_{xz} = \frac{\partial w}{\partial x} + \frac{\partial u}{\partial z} = \theta \left(\frac{\partial \phi}{\partial x} - y\right)$$

$$\gamma_{yz} = \frac{\partial w}{\partial y} + \frac{\partial v}{\partial z} = \theta \left(\frac{\partial \phi}{\partial y} + x\right) \tag{2}$$

The corresponding stresses as given by elasticity theory are

$$\sigma_x = \sigma_y = \sigma_z = \tau_{xy} = 0$$

$$\tau_{xz} = G\gamma_{xz} = G\theta\left(\frac{\partial \phi}{\partial x} - y\right)$$

$$\tau_{yz} = G\gamma_{yz} = G\theta\left(\frac{\partial \phi}{\partial y} + x\right) \tag{3}$$

As pointed out by Timoshenko,[4] from the assumed displacements, there will be no normal stresses acting between the longitudinal fibers of the shaft or in the longitudinal directions of these fibers. At each point in the cross section a condition of pure shear, as defined by the stress tensor of (4) below, exists.

$$\begin{bmatrix} 0 & 0 & \tau_{xz} \\ 0 & 0 & \tau_{yz} \\ \tau_{xz} & \tau_{yz} & 0 \end{bmatrix} \tag{4}$$

From consideration of the equilibrium of forces acting on a rectangular parallelepiped of sides dx, dy, and dz, the equilibrium equations, neglecting body forces, reduce to[5]

$$\frac{\partial \tau_{xz}}{\partial x} + \frac{\partial \tau_{yz}}{\partial y} = 0$$

$$\frac{\partial \tau_{xz}}{\partial z} = 0, \quad \frac{\partial \tau_{yz}}{\partial z} = 0 \tag{5}$$

Equation (3) satisfies the last two conditions of Equation (5).

The vital step in the analysis, according to Den Hartog,[6] is the assumption by Saint-Venant that there is a function $F(x,y)$ such that the stresses may be found from it by differentiation, that is:

$$\tau_{xz} = \frac{\partial F}{\partial y} \quad , \qquad \tau_{yz} = -\frac{\partial F}{\partial x} \tag{6}$$

The expression $F(x,y)$ is called the elastic stress function. Substitution of the expressions of Equations (6) into (3) yields

$$\frac{\partial F}{\partial y} = G\theta\left(\frac{\partial \phi}{\partial x} - y\right), \quad -\frac{\partial F}{\partial x} = G\theta\left(\frac{\partial \phi}{\partial y} + x\right) \tag{7}$$

Differentiating the first expression of Equations (7) with respect to $y$, the second expression with respect to $x$, and subtracting from the first yields the following partial differential equation in terms of the elastic stress function $F$

$$\frac{\partial^2 F}{\partial x^2} + \frac{\partial^2 F}{\partial y^2} = -2G\theta \tag{8}$$

Equation (8) must satisfy the boundary condition that the resultant shearing stress at the boundary is directed along the tangent to the boundary,[7] that is

$$\tau_{xz}\frac{dy}{ds} + \tau_{yz}\left(-\frac{dx}{ds}\right) = 0 \tag{9}$$

where (see Figure 1), $\cos(N,x) = \frac{dy}{ds}$ and $\cos(N,y) = -\frac{dx}{ds}$. In terms of the elastic stress function $F$, Equation (9) becomes

$$\frac{\partial F}{\partial y}\frac{dy}{ds} + \frac{\partial F}{\partial x}\frac{dx}{ds} = \frac{dF}{ds} = 0 \tag{10}$$

Since the total derivative of the elastic stress function F with respect to the boundary distance s is zero, the elastic stress function F is constant along the boundary of the cross section.

The twisting moment T, with reference to Figure 1, is expressed by the double integral

$$T = \int\int (\tau_{yz}\, x - \tau_{xz}\, y)\, dxdy \tag{11}$$

If the constant value of the stress function F on the boundary curve $y = f(x)$ of the cross section is taken equal to zero, as may be done for singly connected boundaries, integration of Equation (11) yields[8]

$$T = 2 \int\int F\, dxdy \tag{12}$$

As Murphy indicates,[9] the actual determination of the stress function as defined by Equation (8) for all but a few relatively simple cross sections becomes difficult, if not impossible, to determine analytically.

Quantitative solutions to the differential Equation (8), however, can be obtained by use of the membrane analogy. Prandtl observed in 1903 that the equation (8) of the elastic stress function is the same as the differential equation for the shape of a stretched membrane, originally flat, which is inflated by air pressure from below. This equation, as derived from the equilibrium of forces when summed in the direction z, is[10]

$$\frac{\partial^2 z}{\partial x^2} + \frac{\partial^2 z}{\partial y^2} = -\frac{p}{s} \tag{13}$$

In Equation (13) z is the deflection of the membrane, p is the pressure acting on the membrane, and s is the surface tension developed in the membrane. Equation (8), the differential equation of elastic torsion, is identical in form to Equation (13) if

$$\frac{p}{s} = 2G\theta \tag{14}$$

If in addition the boundary conditions are satisfied, the deflection z will equal F(x,y), the elastic stress function. In summary, the stress function F(x,y) is represented by the curved surface of the membrane and the contour lines of the surface represent the stress lines of the elastically twisted cross section. The tangent in the xy plane to any contour line of the membrane is in the direction of the resultant shearing stress $\tau$. The stress is proportional to the slope of the stress surface F(x,y). The twisting moment T is equal to twice the volume enclosed by the stress surface.

These characteristics of the membrane analogy have permitted extensive quantitative measurements of the stresses in a twisted bar within the elastic range. Griffith[11] and Hetenyi[12] outline applications of the membrane analogy.

The Sand-Heap Analogy for Plastic Torsion

If the cross section of Figure 1 is twisted beyond the yield point, certain parts of the bar will be deformed plastically. The condition at which

plastic deformation commences is, according to Prager,[13] expressed by

$$I_2 - k^2 = 0 \tag{15}$$

where $I_2$ is the second invariant of the stress tensor. It is independent of the orientation of the coordinate axes. $I_2$ is expressed by (see Reference 14)

$$I_2 = -(\sigma_x\sigma_y + \sigma_y\sigma_z + \sigma_z\sigma_x) + \tau_{xy}^2 + \tau_{yz}^2 + \tau_{zx}^2 \tag{16}$$

The condition of stress in torsion as represented by the stress tensor of (4) produces, when substituted in the condition of plasticity of Equation (15),

$$\tau_{xz}^2 + \tau_{yz}^2 = k^2 = \text{constant} \tag{17}$$

The yield condition of Equation (15) was first postulated by Von Mises[15] but its most widely known physical interpretation is embodied in the octahedral shearing stress theory introduced by Nadai.[16]

The equilibrium equations (5) must be satisfied in the plastic as well as elastic region. As noted by Nadai[17], Equations (5) are satisfied if

$$\tau_{xz} = \frac{\partial F_1(x,y)}{\partial y}, \quad \tau_{yz} = -\frac{\partial F_1(x,y)}{\partial x} \tag{18}$$

in which $F_1(x,y)$ represents the plastic stress function of the cross section. In those regions of the cross section where plastic flow occurs the condition of plasticity of Equation (17), in terms of the plastic stress function, is

$$\left(\frac{\partial F_1}{\partial x}\right)^2 + \left(\frac{\partial F_1}{\partial y}\right)^2 = k^2 \tag{19}$$

The left side of Equation (19) is the square of the largest slope of the surface $F_1$. From the mathematical definition of the gradient, Equation (19) may be expressed as

$$\left|\text{grad } F_1\right| = k = \text{constant} \tag{20}$$

where k is the maximum shearing stress shown in Figure 2.

As in the case of the elastic stress function F, the shearing stresses are directed tangentially to the contour lines of the plastic stress surface. The surface representing this plastic stress function may be thought of as the maximum value that the elastic stress function can attain. The plastic stress function may be considered as a "roof" under which the membrane, geometrically the same as the cross section, expands. When the membrane touches the "roof," the condition of plasticity of Equation (17) is satisfied and plastic yielding begins at that point in the cross section. As the torque is increased, as represented by increasing air pressure on the membrane, the membrane expands and touches more of the "roof." At the limit the membrane fills the entire volume under the roof. The cross section is considered to have attained a fully plastic state. Following the membrane analogy, the torque required to achieve the fully plastic state is equal to twice the volume under the "roof."

The mathematical and physical interpretation of the plastic stress function $F_1(x,y)$ for the case of complete yielding of the entire prismatic bar can be demonstrated by sand heaps covering a plate similar in cross section to the twisted bar. This analogy was first presented by Nadai at

a meeting of the German Society of Applied Mathematics and Mechanics in Marburg, Germany in 1923.

As described by Sadowsky,[18] ..."A plate whose shape is geometrically similar to the cross section of the twisted bar serves as a horizontal tray to hold a heap of dry uniform sand. The heap is to be as big as it is possible to pile by pouring a gentle stream of sand on top of the model, the excessive sand rolling freely down the slopes of the heap and falling off the elevated tray. The maximum-size heap being formed, its volume V is determined by weighing..." The twisting moment T in plastic torsion is now given by the equation

$$T = 2\frac{k}{m} V \tag{21}$$

in which k is the maximum value of the shearing stress in Figure 2 and m is the maximum value of the slope of the lateral surface of the sand heap. In addition, the horizontal lines of the heap, projected vertically down on the supporting tray, give the system of trajectories of the maximum shearing stress k acting upon the cross section.

As pointed out by Murphy,[19] the relative strength of cross sections of different shapes may be determined through use of the sand-heap analogy. It is the purpose of this investigation to evaluate the effect of circular holes, of varying size and location, upon the capability of a circular cross section to sustain plastic torsion. The sand-heap analogy as developed by Nadai and as modified by Sadowsky to include holes will be used.

The Sand-Heap Analogy Applied to Cross Sections with Holes

The twisting moment T, as given by Equation (21) is applicable to cross sections with and without holes. However, in carrying out the experiment it can be visualized that even the presence of a small hole in the cross section will permit an excessively large amount of sand to flow through it. The volume of sand remaining on the tray would not therefore be proportional to the torque required to obtain a fully plastic condition in the cross section.[20]

Therefore, Sadowsky in 1941 modified Nadai's original analogy. If the cross section has holes, similar holes must be made in the supporting tray. In order to prevent the sand from flowing out through these holes, cylinders capable of vertical movement must be inserted into the holes. To hold the tray and to insure vertical travel a device as shown in Figure 4 and Plate 1 was constructed. Trays A and B are geometrically similar to the cross section under investigation.

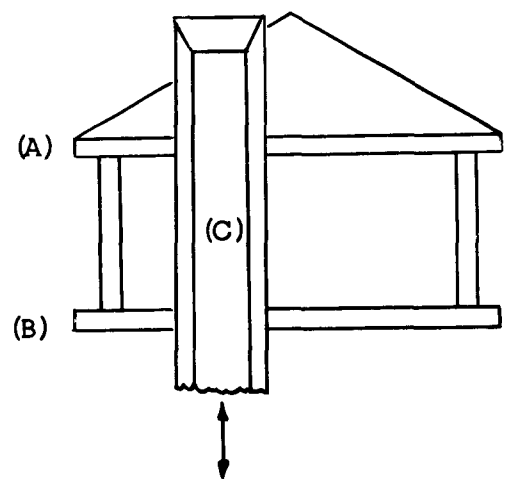


Figure 4. Model for Sand-Heap Analysis of Cross Section with Hole

It is important that the top of cylinder C be kept horizontal and its inner conical edges be sharpened so that a grain of sand placed on this edge will fall through the cylinder.

At the beginning of the experiment, the cylinder C is moved into a position as high as possible and a maximum sand heap is formed on the upper tray only. At this stage the cylinder is free of sand standing above the sand heap. After the maximum heap is formed, as shown in Figure 4, the cylinder is gradually lowered. At a certain position the top of the cylinder will reach the surface of the heap and the sand will commence to fall through the top of the cylinder. The lowering of the cylinder will continue until the brim of the cylinder is completely submerged in the sand. In the final position, the cylinder is at the maximum height at which no part of its lateral surface will protrude from the heap and be visibly exposed. Although extremely complicated mathematical surfaces may be formed in three-dimensional sand heaps, the geometric problem solves itself through the medium of the sand. This procedure applies as well to cross sections with more than one hole.

Designate $V_o$ as the volume of the sand remaining on the tray after the cylinder or cylinders have been lowered. Let $S_1$, $S_2$ ... $S_n$ be the areas of the holes, with depths $h_1$, $h_2$, ... $h_n$ - as measured from the level of the tray up to the top of the cylindrical opening. Then the volume V as defined by Equation (21) is

$$V = V_o + S_1 h_1 + S_2 h_2 + \ldots S_n h_n \tag{22}$$

The twisting moment T is therefore given by

$$T = 2 \frac{k}{m} (V_o + S_1 h_1 + S_2 h_2 + \ldots S_n h_n) \tag{23}$$

The mathematical derivation of Equation (23) follows. Consider the twisted prismatic cross section with a hole shown in Figure 5.

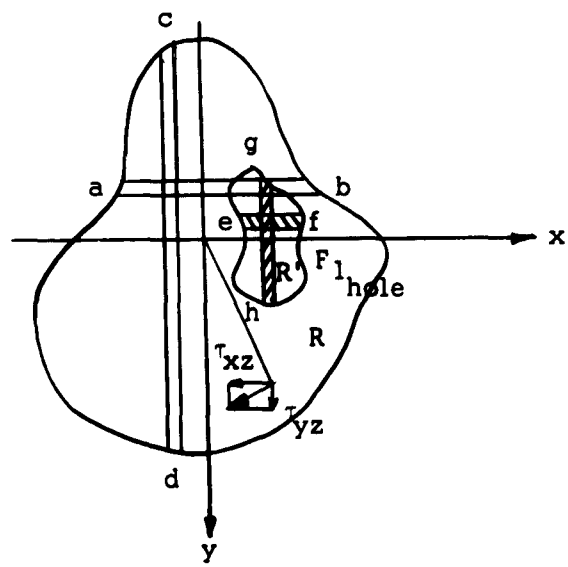


Figure 5. Two-Dimensional View, Prismatic Cross Section with Hole.

R is the entire cross-sectional area including the region R' of the hole.

The twisting moment T is therefore

$$T = \iint_{R(x,y)} (\tau_{yz} x - \tau_{xz} y)\, dx\, dy - \iint_{R'(x,y)} (\tau_{yz} x - \tau_{xz} y)\, dx\, dy \tag{24}$$

Defining the shearing stresses in terms of the plastic stress function $F_1$, one obtains

$$\tau_{xz} = \frac{k}{m}\frac{\partial F_1}{\partial y} \quad \text{and} \quad \tau_{yz} = -\frac{k}{m}\frac{\partial F_1}{\partial x} \tag{25}$$

Substituting these expressions for shearing stresses into Equation (24) and noting that k and m are constants, one finds

$$T = -\frac{k}{m}\iint_R \left(\frac{\partial F_1}{\partial x}x + \frac{\partial F_1}{\partial y}y\right) dx\,dy + \frac{k}{m}\iint_{R'} \left(\frac{\partial F_1}{\partial x}x + \frac{\partial F_1}{\partial y}y\right) dx\,dy$$

Consider the first integral over the region R with the limits of integration indicated from Figure 5,

$$-\frac{k}{m}\iint_R \left(\frac{\partial F_1}{\partial x}x + \frac{\partial F_1}{\partial y}y\right) dx\,dy = -\frac{k}{m}\left\{\int_c^d \left[\int_a^b \frac{\partial F_1}{\partial x}x\,dx\right] dy\right.$$

$$\left. + \int_a^b \left[\int_c^d \frac{\partial F_1}{\partial y}y\,dy\right] dx\right\} = -\frac{k}{m}\left\{\int_c^d \left[xF_1\Big|_a^b - \int_a^b F_1 dx\right] dy\right.$$

$$\left. + \int_a^b \left[yF_1\Big|_c^d - \int_c^d F_1 dy\right] dx\right\} = -\frac{k}{m}\left\{\int_c^d \left[x_b F_{1_b} - x_a F_{1_a}\right] dy\right.$$

$$\left. - \int_c^d \int_a^b F_1\,dx\,dy + \int_a^b \left[y_d F_d - y_c F_{1_c}\right] dx - \int_a^b \int_c^d F_1\,dy\,dx\right\}$$

However, $F_{1_a} = F_{1_b} = F_{1_c} = F_{1_d} = F_1$ outside; therefore, the first integral equals

$$\frac{k}{m}\left\{2\int_a^b \int_c^d F_1\,dy\,dx - F_{1_a}\int_c^d (x_b - x_a)\,dy - F_{1_a}\int_a^b (y_d - y_c)\,dx\right\}$$

But $\int_c^d (x_b - x_a)\,dy = \int_a^b (y_d - y_c)\,dx = A$, the area of region R.

Therefore, the first integral equals

$$\frac{k}{m}\left\{2\int_a^b\int_c^d F_1\,dy\,dx - 2\,F_{1_{outside}}\,A\right\}$$

Taking $F_{1_{outside}}$ equal to zero, which is the height of the base of the sand heap, one obtains from the first integral

$$2\frac{k}{m}\int_a^b\int_c^d F_1\,dy\,dx$$

In a similar manner the second integral over R' is

$$\frac{k}{m}\iint_{R_1}\left(\frac{\partial F_1}{\partial x}x + \frac{\partial F_1}{\partial y}y\right)dx\,dy = -2\frac{k}{m}\int_e^f\int_g^h F_1\,dy\,dx + 2\frac{k}{m}\,F_{1_{hole}}\,A'$$

where A' is the area of the region R'. Since the top of the region R' is made open, the height of the sand heap in R' is zero and $F_1$ is zero over the region R'. The second integral therefore equals $2\frac{k}{m}F_{1_{hole}}A'$.

The twisting moment T is

$$T = 2\frac{k}{m}\left\{\int_a^b\int_c^d F_1\,dy\,dx + F_{1_{hole}}A'\right\} \tag{26}$$

Since $F_1$ is equal to the height of the sand heap, the terms in braces are the volume of the sand on the tray $V_o$ and the volume enclosing the hole, respectively. If $F_{1_{hole}}$ is designated as $h_1$, the height of the

sand heap at the hole, it follows that the twisting moment T as expressed by Equation (23) and Equation (26) are equal for a cross section with one hole. For this case

$$T = 2\frac{k}{m}\left\{V_o + h_1 S_1\right\} \tag{27}$$

This relationship will be used directly for this analysis.

# CHAPTER III

## DIMENSIONAL ANALYSIS

In order for the results to be of general application, use was made of the Buckingham $\pi$ theorem to present the experimental results in non-dimensional form. The Buckingham $\pi$ theorem states that the number of dimensionless and independent quantities required to express a relationship among the variables in any phenomenon is equal to the number of quantities involved minus the number of dimensions in which these quantities may be measured. That is, $s_1 = n - b$, where $s_1$ is the number of $\pi$ terms, n is the total number of quantities involved, and b is the number of basic dimensions.[21]

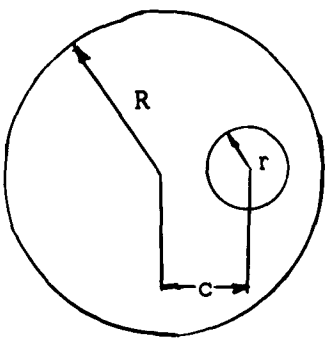


Figure 6. Two-Dimensional View, Circular Cross Section with Circular Hole.

For this case (see Figure 6) choose

$$T = f(k, R, r, c) \tag{1a}$$

Dimensionally

$T$ = twisting moment $\doteq (FL)$

$k$ = maximum shearing stress $\doteq (FL^{-2})$

$R$ = radius of circular cross section $\doteq (L)$

$r$ = radius of circular hole $\doteq (L)$

$c$ = distance from center of hole to center of cross section $\doteq (L)$

Since

$$s_1 = n - b = 5 - 2 = 3$$

Three $\pi$ terms are necessary to describe twisting moment behavior of the cross section in plastic torsion.

From Equation (1a) where $\doteq$ denotes dimensional equivalence

$$1 \doteq (T)^a (r)^b (c)^c (R)^d (k)^e$$

Dimensionally

$$1 \doteq (FL)^a (L)^b (L)^c (L)^d (FL^{-2})^e$$

F: $0 \doteq a + e$

L: $0 \doteq a + b + c + d - 2e$

Since there are two independent equations in five unknowns, evaluate d and e in terms of a, b, and c:

$$e = -a$$

$$d = -3a - b - c$$

Therefore

$$1 \doteq (T)^a (r)^b (c)^c (R)^{-3a-b-c} (k)^{-a}$$

$$1 \doteq \left(\frac{T}{R^3 k}\right)^a \left(\frac{r}{R}\right)^b \left(\frac{c}{R}\right)^c$$

Expressed functionally,

$$\left(\frac{T}{R^3 k}\right) = f\left[\left(\frac{r}{R}\right), \left(\frac{c}{R}\right)\right]$$

The experimental results will therefore be expressed in the three non-dimensional $\pi$ terms of $\frac{T}{R^3 k}$, $\frac{r}{R}$, $\frac{c}{R}$.

# CHAPTER IV

## EXPERIMENTAL PROCEDURES

Prior to investigating the effect of a circular hole on the plastic strength in torsion of a circular section, sections whose plastic stress function equation were known were investigated. Circular, square, and rectangular cross sections were tested to verify experimental techniques. The results are contained in the Appendix.

The sand used was Ottawa sand, American Society Testing Materials designation C-190, produced by the Ottawa Silica Company, Ottawa, Illinois. Of uniform composition its specific volume was determined as the arithmetic mean of ten measurements to be 39.398 cubic inches per kilogram.

Its slope m was determined to be 0.636. The volume $V_o$ was determined by measuring the mass of sand remaining on the tray. The height of the circular cylinder h was also measured.

The value of $\frac{T}{kR^3}$ was determined using Equation (27) in terms of the sand-heap analogy. In order to measure the effect of varying size and location of the hole, the radius of the hole was varied as follows: r = 0.25 in., 0.50 in., 0.75 in., 0.875 in., 1.125 in., 1.313 in., 1.50 in., 1.750 in., 2.0 in., 2.250 in., and 3.313 in. The radius of the circular cross section R was constant at six in. The offset c varied as follows: c = 1.2 in., 2.4 in., 3.6 in., 4.8 in., and 6.0 in.

Plates 1 through 8 (see Appendix) picture the model and several sand heaps formed.

# CHAPTER V

## RESULTS AND CONCLUSIONS

Results are shown in Figures 7 and 8. The data for each size hole and keyway are tabulated in Tables 1 through 11. Figure 7 shows the maximum strength in torsion when the circular shaft has an interior hole. Figure 8 predicts the maximum strength in torsion of a circular shaft with a keyway. It is noted in the tables that when the offset distance c has increased to where the hole has become a keyway, the region becomes singly connected and the stress function is taken as zero about the keyway circumference.

The curves are used in the following manner. Knowing the size r, location c, and radius of the cross section R, the value $\frac{T}{kR^3}$ is determined if $\frac{r}{R} \leq 0.56$. The yield stress k is determined from the shearing stress-strain curve of the material. The value of T, the maximum strength in torsion, is then determined in the appropriate dimensions of k and R.

With the exception of mild steel, which behaves very nearly as a perfectly plastic material at the beginning of strain hardening,[22] the material possessing the characteristics of Figure 2 are rarely found. However, depending on the degree of conservativeness desired in the design and the specific material characteristics, an idealization of the shearing stress-strain curve can be made to determine the value k.

The above analysis assumes that the shearing strains remain small in order that no components of normal stresses act in sections normal or parallel to the axis of the bar.[23]

Mindful of these assumptions and resulting limitations, Figures 7 and 8 can be used in predicting the maximum strength in torsion of circular cross sections with holes.

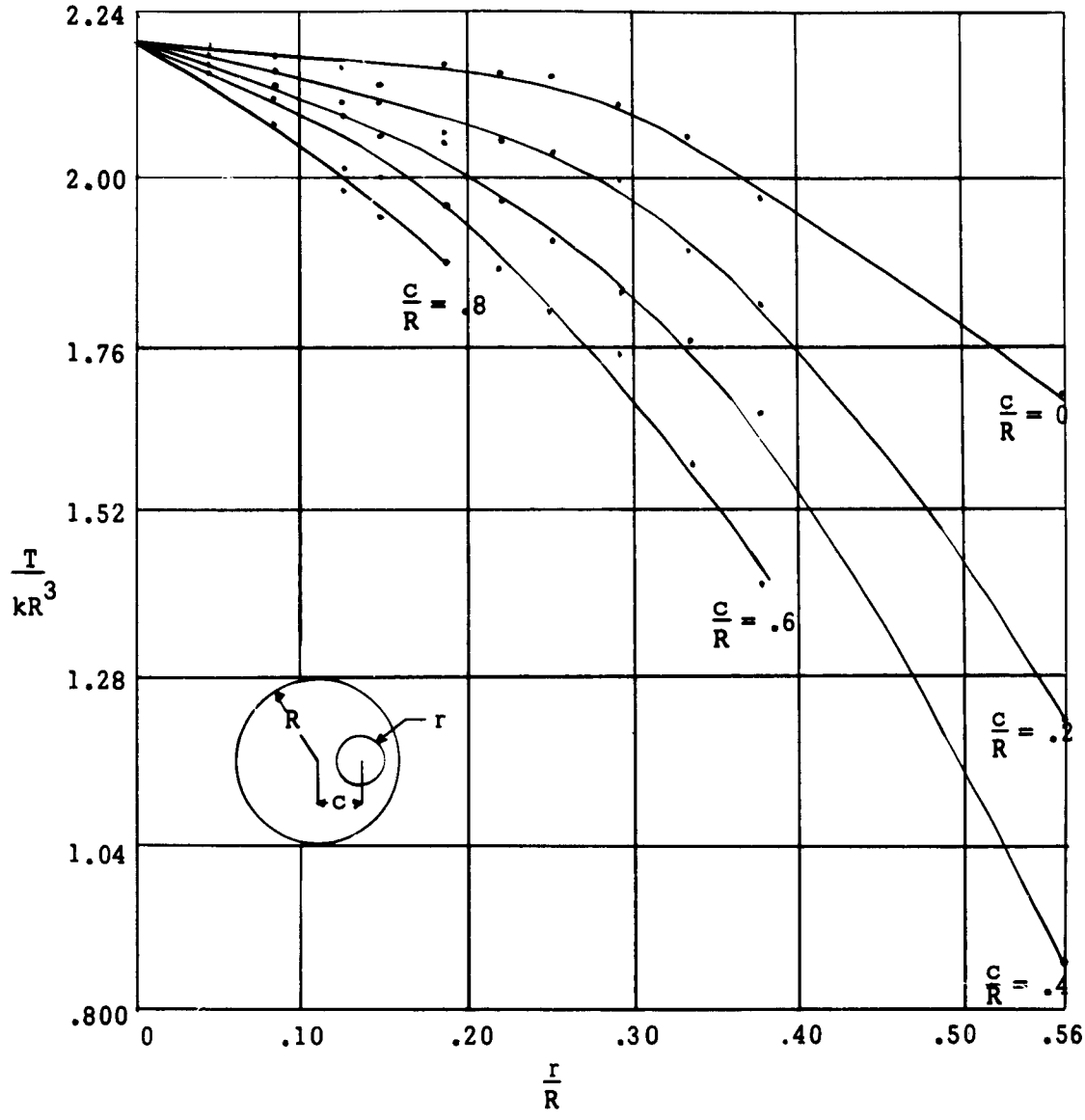


Figure 7. Maximum Strength in Torsion-Circular Bar with Hole.

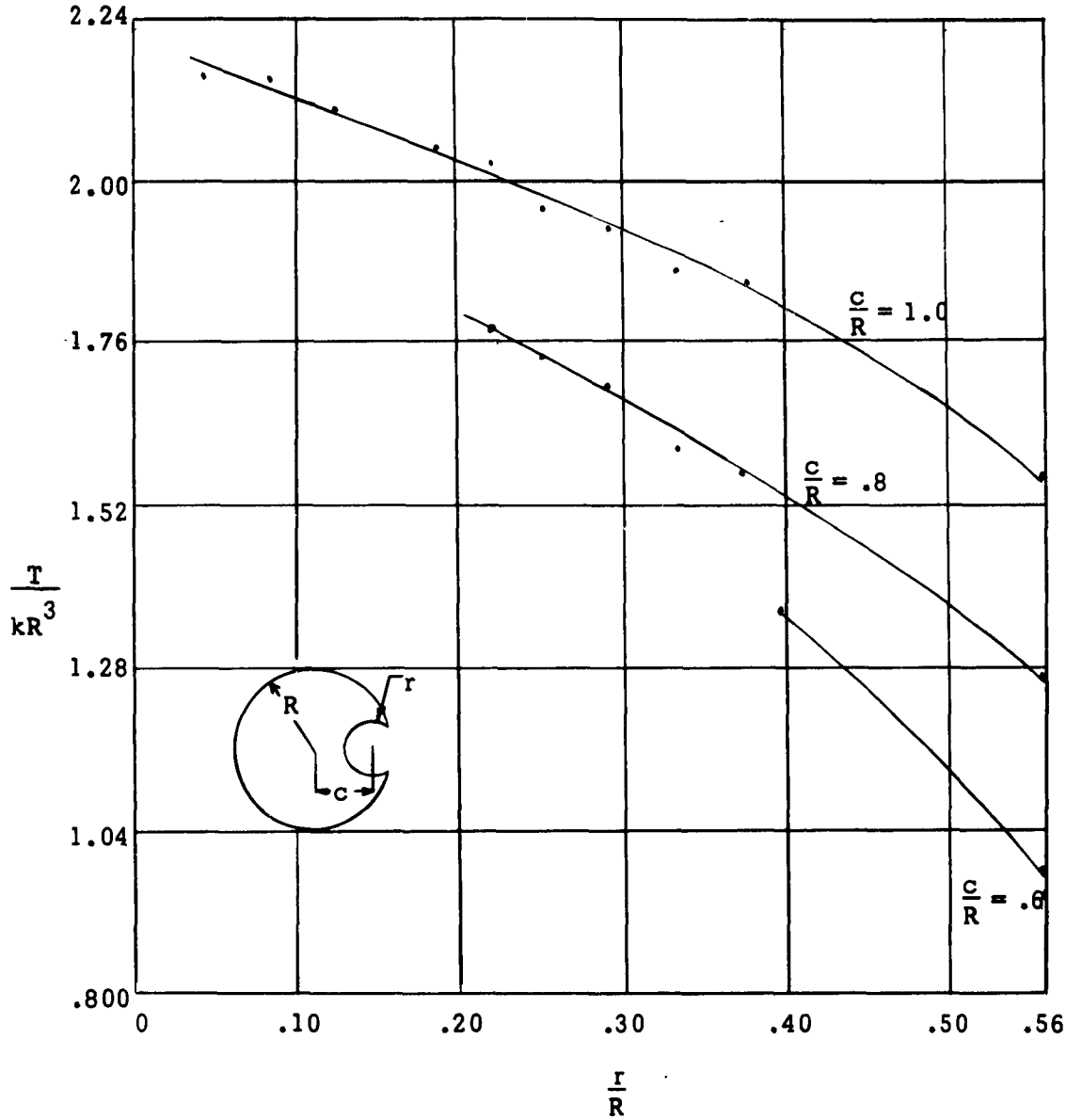


Figure 8. Maximum Strength in Torsion-Circular Bar with Keyway.

Table 1. Experimental Results,* $\frac{r}{R} = 0, \frac{r}{R} = 0.0417$, r = 0.25"

| $\frac{c}{R}$ | Mass (gms) | $V_o$ ($in^3$) | h (in) | hs ($in^3$) | $V_o$+hs | $\frac{T}{kR^3}$ |
|---|---|---|---|---|---|---|
| no hole | 3850 | 151.682 | | | 151.682 | |
| | 3821 | 150.540 | | | 150.540 | 2.1976 |
| | 3824 | 150.658 | | | 150.658 | |
| 0 | 3712 | 146.245 | 3.250 | 0.638 | 146.883 | |
| | 3726 | 146.797 | 3.156 | 0.619 | 147.416 | 2.1464 |
| | 3740 | 147.349 | 3.156 | 0.619 | 147.968 | |
| 0.2 | 3776 | 148.767 | 2.686 | 0.528 | 149.295 | |
| | 3778 | 148.846 | 2.500 | 0.491 | 149.337 | 2.184 |
| | 3828 | 150.816 | 2.906 | 0.570 | 151.386 | |
| 0.4 | 3827 | 150.776 | 2.031 | 0.399 | 151.175 | |
| | 3774 | 148.688 | 1.906 | 0.374 | 149.062 | 2.1816 |
| | 3777 | 148.806 | 2.013 | 0.399 | 149.205 | |
| 0.6 | 3745 | 147.546 | 1.188 | 0.233 | 147.779 | |
| | 3762 | 148.136 | 1.250 | 0.246 | 148.382 | 2.1672 |
| | 3817 | 150.382 | 1.219 | 0.239 | 150.406 | |
| 0.8 | 3744 | 147.506 | 0.500 | 0.098 | 147.614 | |
| | 3772 | 148.609 | 0.594 | 0.116 | 148.725 | 2.168 |
| | 3812 | 150.185 | 0.625 | 0.122 | 150.307 | |
| 1.0 | 3747 | 147.624 | | | | |
| | 3768 | 148.452 | | | | 2.1504 |
| | 3732 | 147.033 | | | | |

* All calculations on Marchant Model SKA Desk Calculator.

Table 2. Experimental Results, $\frac{r}{R} = 0.0833$, r = 0.50 in.

| $\frac{c}{R}$ | Mass (gms) | $V_o$ ($in^3$) | h (in) | hs ($in^3$) | $V_o$+hs | $\frac{T}{kR^3}$ |
|---|---|---|---|---|---|---|
| 0 | 3732 | 147.033 | 3.219 | 2.528 | 149.561 | |
| | 3739 | 147.309 | 3.187 | 2.503 | 149.812 | 2.167 |
| | 3672 | 144.670 | 3.157 | 2.480 | 147.150 | |
| 0.2 | 3732 | 147.033 | 2.469 | 1.939 | 148.972 | |
| | 3732 | 147.033 | 2.594 | 2.037 | 149.070 | 2.174 |
| | 3753 | 147.861 | 2.531 | 1.988 | 149.849 | |
| 0.4 | 3682 | 145.063 | 1.844 | 1.448 | 146.511 | |
| | 3665 | 144.394 | 1.781 | 1.399 | 145.793 | 2.150 |
| | 3707 | 146.048 | 1.875 | 1.473 | 147.521 | |
| 0.6 | 3701 | 145.812 | 1.157 | 0.909 | 146.721 | |
| | 3647 | 143.685 | 1.157 | 0.909 | 144.594 | 2.122 |
| | 3679 | 144.945 | 1.188 | 0.933 | 145.878 | |
| 0.8 | 3541 | 139.508 | 0.427 | 0.335 | 139.843 | |
| | 3621 | 142.660 | 0.406 | 0.319 | 142.979 | 2.079 |
| | 3687 | 145.260 | 0.379 | 0.295 | 145.555 | |
| 1.0 | 3737 | 147.230 | | | | |
| | 3739 | 147.309 | | | | 2.148 |
| | 3757 | 148.018 | | | | |

Table 3. Experimental Results, $\frac{r}{R} = 0.125$, r = 0.75 in.

| $\frac{c}{R}$ | Mass (gms) | $V_o$ ($in^3$) | h (in) | hs ($in^3$) | $V_o + hs$ | $\frac{T}{kR^3}$ |
|---|---|---|---|---|---|---|
| 0 | 3637 | 143.290 | 3.000 | 5.301 | 148.591 | |
| | 3625 | 142.818 | 3.031 | 5.356 | 148.174 | 2.164 |
| | 3652 | 143.881 | 3.000 | 5.301 | 149.182 | |
| 0.2 | 3597 | 141.715 | 2.281 | 4.031 | 145.746 | |
| | 3572 | 140.730 | 2.156 | 3.801 | 144.531 | 2.107 |
| | 3548 | 139.784 | 2.313 | 4.087 | 143.871 | |
| 0.4 | 3572 | 140.730 | 1.594 | 2.817 | 143.547 | |
| | 3586 | 141.281 | 1.594 | 2.817 | 144.098 | 2.089 |
| | 3550 | 139.863 | 1.625 | 2.872 | 142.735 | |
| 0.6 | 3515 | 138.484 | 0.875 | 1.546 | 140.030 | |
| | 3452 | 136.002 | 0.938 | 1.658 | 137.660 | 2.010 |
| | 3422 | 134.820 | 0.906 | 1.601 | 136.421 | |
| 0.8 | 3452 | 136.002 | 0.188 | 0.332 | 136.334 | |
| | 3397 | 133.835 | 0.219 | 0.387 | 134.222 | 1.982 |
| | 3492 | 137.578 | 0.219 | 0.387 | 137.965 | |
| 1.0 | 3664 | 144.352 | | | | |
| | 3614 | 142.384 | | | | 2.096 |
| | 3687 | 145.260 | | | | |

Table 4. Experimental Results, $\frac{r}{R} = 0.146$, r = 0.875 in.

| $\frac{c}{R}$ | Mass (gms) | $V_o$ ($in^3$) | h (in) | hs ($in^3$) | $V_o + hs$ | $\frac{T}{kR^3}$ |
|---|---|---|---|---|---|---|
| 0 | 3520 | 138.681 | 2.969 | 7.141 | 145.822 | |
| | 3577 | 140.926 | 2.875 | 6.916 | 147.842 | 2.1334 |
| | 3529 | 139.034 | 2.875 | 6.916 | 145.950 | |
| 0.2 | 3572 | 140.730 | 2.156 | 5.186 | 145.916 | |
| | 3560 | 140.257 | 2.344 | 5.638 | 145.895 | 2.120 |
| | 3538 | 139.390 | 2.344 | 5.638 | 145.028 | |
| 0.4 | 3542 | 139.948 | 1.531 | 3.683 | 143.631 | |
| | 3450 | 135.923 | 1.594 | 3.834 | 139.757 | 2.060 |
| | 3480 | 137.105 | 1.656 | 3.983 | 141.088 | |
| 0.6 | 3409 | 134.308 | 0.937 | 2.254 | 136.562 | |
| | 3467 | 136.593 | 0.937 | 2.254 | 138.847 | 2.006 |
| | 3444 | 135.687 | 0.906 | 2.180 | 137.867 | |
| 0.8 | 3442 | 135.608 | 0.188 | 0.452 | 136.060 | |
| | 3352 | 132.062 | 0.188 | 0.452 | 132.514 | 1.942 |
| | 3340 | 131.590 | 0.188 | 0.452 | 131.635 | |
| 1.0 | 3635 | 143.212 | | | | |
| | 3567 | 140.533 | | | | 2.074 |
| | 3645 | 143.606 | | | | |

Table 5. Experimental Results, $\frac{r}{R} = 0.188$, r = 1.125 in.

| $\frac{c}{R}$ | Mass (gms) | $V_o$ ($in^3$) | h (in) | hs ($in^3$) | $V_o + hs$ | $\frac{T}{kR^3}$ |
|---|---|---|---|---|---|---|
| 0 | 3496 | 137.735 | 2.938 | 11.681 | 149.416 | |
| | 3477 | 136.987 | 2.938 | 11.681 | 148.668 | 2.166 |
| | 3472 | 136.790 | 2.875 | 11.431 | 148.221 | |
| 0.2 | 3502 | 137.972 | 2.500 | 9.940 | 147.912 | |
| | 3527 | 138.956 | 2.500 | 9.940 | 148.896 | 2.145 |
| | 3432 | 135.214 | 2.500 | 9.940 | 145.154 | |
| 0.4 | 3419 | 134.702 | 1.563 | 6.214 | 140.916 | |
| | 3492 | 137.578 | 1.594 | 6.338 | 143.916 | 2.067 |
| | 3426 | 134.978 | 1.531 | 6.087 | 141.065 | |
| 0.6 | 3394 | 133.717 | 0.750 | 2.982 | 136.689 | |
| | 3352 | 132.062 | 0.718 | 2.855 | 134.917 | 1.965 |
| | 3310 | 130.407 | 0.718 | 2.855 | 133.262 | |
| 0.8 | 3292 | 129.698 | 0.0312 | 0.124 | 129.822 | |
| | 3294 | 129.777 | 0.0312 | 0.124 | 129.901 | 1.884 |
| | 3257 | 128.319 | 0.0312 | 0.124 | 128.443 | |
| 1.0 | 3522 | 138.760 | | | | |
| | 3602 | 141.911 | | | | 2.049 |
| | 3592 | 141.517 | | | | |

Table 6. Experimental Results, $\frac{r}{R} = 0.219$, r = 1.313 in.

| $\frac{c}{R}$ | Mass (gms) | $V_o$ ($in^3$) | h (in) | hs ($in^3$) | $V_o + hs$ | $\frac{T}{kR^3}$ |
|---|---|---|---|---|---|---|
| 0 | 3384 | 133.323 | 2.656 | 14.385 | 147.708 | |
| | 3362 | 132.456 | 2.750 | 14.894 | 147.350 | 2.150 |
| | 3385 | 133.362 | 2.687 | 14.553 | 147.915 | |
| 0.2 | 3285 | 129.422 | 2.031 | 11.000 | 140.422 | |
| | 3331 | 131.235 | 2.031 | 11.000 | 142.235 | 2.056 |
| | 3297 | 129.895 | 2.031 | 11.000 | 140.895 | |
| 0.4 | 3266 | 128.674 | 1.406 | 7.615 | 136.289 | |
| | 3237 | 127.531 | 1.406 | 7.615 | 135.146 | 1.972 |
| | 3232 | 127.334 | 1.406 | 7.615 | 134.949 | |
| 0.6 | 3182 | 125.364 | 0.656 | 3.553 | 128.917 | |
| | 3126 | 123.158 | 0.656 | 3.553 | 126.711 | 1.869 |
| | 3197 | 125.955 | 0.687 | 3.553 | 129.508 | |
| 0.8 | 3097 | 122.016 | | | | |
| | 3132 | 123.395 | | | | 1.791 |
| | 3137 | 123.592 | | | | |
| 1.0 | 3564 | 140.414 | | | | |
| | 3506 | 138.129 | | | | 2.026 |
| | 3519 | 138.646 | | | | |

Table 7. Experimental Results, $\frac{r}{R} = 0.250$, r = 1.500 in.

| $\frac{c}{R}$ | Mass (gms) | $V_o$ ($in^3$) | h (in) | hs ($in^3$) | $V_o$+hs | $\frac{T}{kR^3}$ |
|---|---|---|---|---|---|---|
| 0 | 3292 | 129.699 | 2.625 | 18.555 | 148.254 | |
| | 3275 | 129.028 | 2.719 | 19.220 | 148.250 | 2.152 |
| | 3262 | 128.516 | 2.594 | 18.336 | 146.852 | |
| 0.2 | 3205 | 126.271 | 2.063 | 14.583 | 140.854 | |
| | 3177 | 125.167 | 2.000 | 14.137 | 139.304 | 2.044 |
| | 3209 | 126.428 | 2.063 | 14.583 | 141.011 | |
| 0.4 | 3117 | 122.804 | 1.313 | 9.281 | 132.085 | |
| | 3096 | 121.976 | 1.344 | 9.500 | 131.476 | 1.912 |
| | 3087 | 121.622 | 1.219 | 8.617 | 130.239 | |
| 0.6 | 3107 | 122.409 | 0.656 | 4.637 | 127.046 | |
| | 3042 | 119.849 | 0.594 | 4.199 | 124.048 | 1.810 |
| | 2994 | 117.958 | 0.563 | 3.980 | 121.938 | |
| 0.8 | 3022 | 119.061 | | | | |
| | 3032 | 119.455 | | | | 1.745 |
| | 3069 | 120.912 | | | | |
| 1.0 | 3414 | 134.505 | | | | |
| | 3395 | 133.756 | | | | 1.960 |
| | 3442 | 135.608 | | | | |

Table 8. Experimental Results, $\frac{r}{R} = 0.292$, $r = 1.750$

| $\frac{c}{R}$ | Mass (gms) | $V_o$ ($in^3$) | h (in) | hs ($in^3$) | $V_o + hs$ | $\frac{T}{kR^3}$ |
|---|---|---|---|---|---|---|
| 0 | 3054 | 120.321 | 2.406 | 23.149 | 143.470 | |
| | 3098 | 122.055 | 2.500 | 24.053 | 146.108 | 2.100 |
| | 3028 | 119.297 | 2.469 | 23.755 | 143.052 | |
| 0.2 | 2987 | 117.682 | 1.844 | 17.741 | 135.423 | |
| | 3071 | 120.991 | 1.865 | 17.944 | 138.935 | 1.998 |
| | 3022 | 119.061 | 1.906 | 18.338 | 137.399 | |
| 0.4 | 2917 | 114.924 | 1.094 | 10.526 | 125.450 | |
| | 2954 | 116.382 | 1.094 | 10.526 | 126.908 | 1.838 |
| | 2943 | 115.948 | 1.094 | 10.526 | 126.474 | |
| 0.6 | 2909 | 114.609 | 0.500 | 4.811 | 119.420 | |
| | 2922 | 115.121 | 0.500 | 4.811 | 119.932 | 1.745 |
| | 2929 | 115.397 | 0.500 | 4.811 | 120.208 | |
| 0.8 | 2968 | 116.933 | | | | |
| | 2966 | 118.036 | | | | 1.700 |
| | 2928 | 115.357 | | | | |
| 1.0 | 3358 | 132.298 | | | | |
| | 3370 | 132.771 | | | | 1.930 |
| | 3364 | 132.535 | | | | |

Table 9. Experimental Results, $\frac{r}{R} = 0.333$, r = 2.0 in.

| $\frac{c}{R}$ | Mass (gms) | $V_o$ ($in^3$) | h (in) | hs ($in^3$) | $V_o$+hs | $\frac{T}{kR^3}$ |
|---|---|---|---|---|---|---|
| 0 | 2837 | 111.772 | 2.281 | 28.664 | 140.436 | |
| | 2824 | 111.260 | 2.250 | 28.274 | 139.534 | 2.038 |
| | 2823 | 111.221 | 2.281 | 28.664 | 139.885 | |
| 0.2 | 2793 | 110.039 | 1.687 | 21.200 | 131.239 | |
| | 2742 | 108.029 | 1.687 | 21.200 | 129.229 | 1.893 |
| | 2741 | 107.990 | 1.719 | 21.602 | 129.592 | |
| 0.4 | 2789 | 109.881 | 1.000 | 12.566 | 122.447 | |
| | 2772 | 109.221 | 1.000 | 12.566 | 121.787 | 1.772 |
| | 2758 | 108.660 | 0.969 | 12.177 | 120.837 | |
| 0.6 | 2692 | 106.059 | 0.375 | 4.712 | 110.771 | |
| | 2659 | 104.759 | 0.344 | 4.323 | 109.082 | 1.596 |
| | 2667 | 105.074 | 0.313 | 3.933 | 109.007 | |
| 0.8 | 2789 | 109.881 | | | | |
| | 2838 | 111.812 | | | | 1.613 |
| | 2807 | 110.590 | | | | |
| 1.0 | 3287 | 129.501 | | | | |
| | 3254 | 128.201 | | | | 1.869 |
| | 3231 | 127.295 | | | | |

Table 10. Experimental Results, $\frac{r}{R} = 0.375$, r = 2.25 in.

| $\frac{c}{R}$ | Mass (gms) | $V_o$ ($in^3$) | h (in) | hs ($in^3$) | $V_o$+hs | $\frac{T}{kR^3}$ |
|---|---|---|---|---|---|---|
| 0 | 2637 | 103.893 | 2.156 | 34.290 | 138.183 | |
| | 2597 | 102.317 | 2.188 | 34.799 | 137.116 | 1.973 |
| | 2612 | 102.908 | 2.158 | 34.322 | 137.222 | |
| 0.2 | 2594 | 102.198 | 1.469 | 23.364 | 125.562 | |
| | 2570 | 101.253 | 1.469 | 23.364 | 124.617 | 1.820 |
| | 2571 | 101.292 | 1.469 | 23.364 | 124.656 | |
| 0.4 | 2527 | 99.559 | 0.906 | 14.409 | 113.968 | |
| | 2562 | 100.938 | 0.906 | 14.409 | 115.347 | 1.670 |
| | 2545 | 100.268 | 0.906 | 14.409 | 114.677 | |
| 0.6 | 2392 | 94.240 | 0.094 | 1.495 | 95.898 | 1.395 |
| | 2396 | 94.398 | 0.094 | 1.495 | 95.893 | |
| 0.8 | 2747 | 108.226 | | | | |
| | 2740 | 107.950 | | | | 1.575 |
| | 2750 | 108.345 | | | | |
| 1.0 | 3223 | 126.980 | | | | |
| | 3232 | 127.334 | | | | 1.849 |
| | 3212 | 126.546 | | | | |

Table 11. Experimental Results, $\frac{r}{R} = 0.5522$, $r = 3.313$ in.

| $\frac{c}{R}$ | Mass (gms) | $V_o$ ($in^3$) | h (in) | hs ($in^3$) | $V_o$+hs | $\frac{T}{kR^3}$ |
|---|---|---|---|---|---|---|
| 0 | 1626 | 64.061 | 1.500 | 51.723 | 115.784 | |
| | 1645 | 64.810 | 1.500 | 51.723 | 116.533 | 1.752 |
| | 1654 | 65.164 | 1.500 | 51.723 | 116.887 | |
| 0.2 | 1562 | 61.540 | 0.625 | 21.551 | 83.091 | |
| | 1582 | 62.328 | 0.625 | 21.551 | 83.879 | 1.222 |
| | 1605 | 63.234 | 0.625 | 21.551 | 84.785 | |
| 0.4 | 1452 | 57.206 | 0.125 | 4.310 | 61.516 | |
| | 1415 | 55.748 | 0.125 | 4.310 | 60.058 | 0.880 |
| | 1405 | 55.354 | 0.125 | 4.310 | 59.664 | |
| 0.6 | 1727 | 68.040 | | | | |
| | 1704 | 67.134 | | | | 0.972 |
| | 1736 | 68.395 | | | | |
| 0.8 | 2192 | 86.360 | | | | |
| | 2221 | 87.503 | | | | 1.270 |
| | 2232 | 87.936 | | | | |
| 1.0 | 2723 | 107.281 | | | | |
| | 2730 | 107.557 | | | | 1.566 |
| | 2737 | 107.832 | | | | |

# APPENDIX

Plate 1 Model, $r/R = .375$, $c/R = 0$

Plate 2 Sand Heap, $r/R = .375$, $c/R = 0$

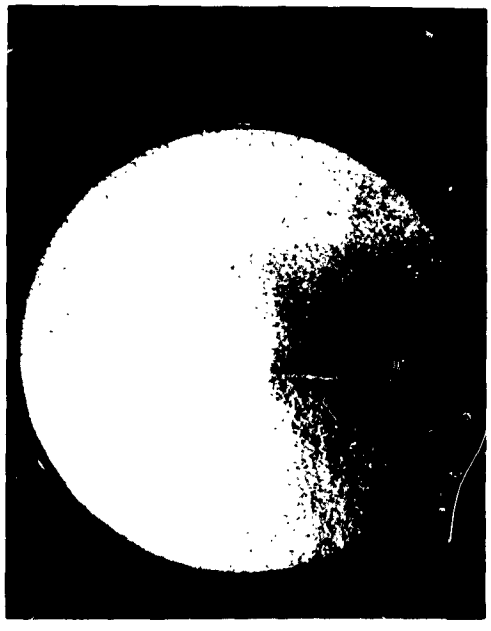

Plate 3 Sand Heap, $r/R = 0$, $c/R = 0$

Plate 4 Sand Heap, $r/R = .219$, $c/R = 1.0$

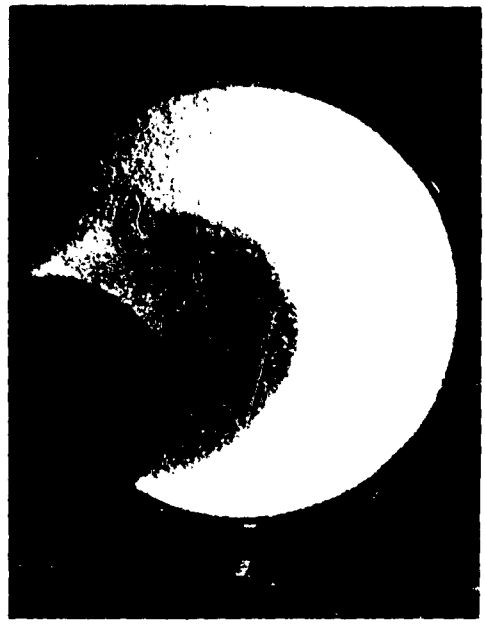

Plate 5 Sand Heap, $^{r}/_{R}$ .552, $^{c}/_{R}$ = 1.0

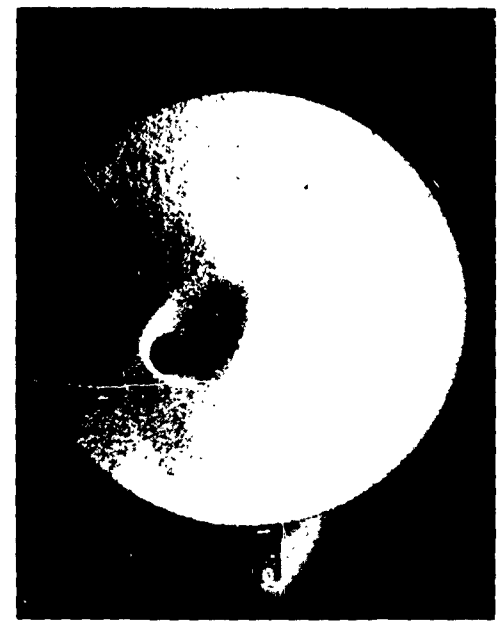

Plate 6 Sand Heap, $^{r}/_{R}$ = .0833, $^{c}/_{R}$ = .4

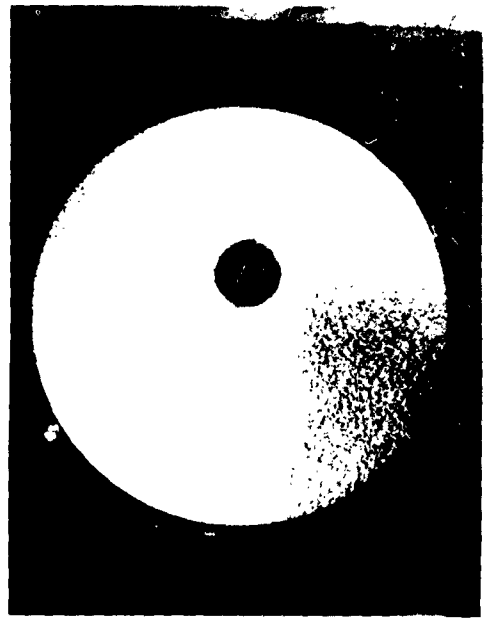

Plate 7 Sand Heap, $^{r}/_{R}$ = .292, $^{c}/_{R}$ = .2

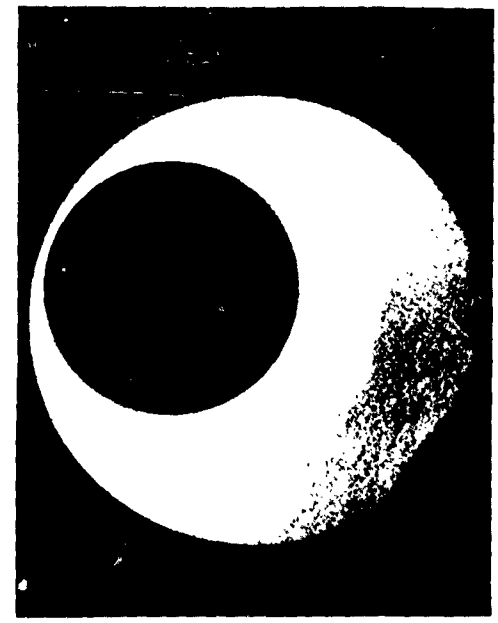

Plate 8 Sand Heap, $^{r}/_{R}$ = .552, $^{c}/_{R}$ = .4

## CALIBRATION EXPERIMENTS

The plastic stress functions for such singly connected regions as a circular, square, and rectangular cross section can readily be predicted mathematically. The plastic stress function for a circular section is the surface of a right circular cone and its strength in plastic torsion is equal to twice the volume of a right circular cone whose slope is equal to the yield stress k. Similarly, the plastic strength of a square bar would equal twice the volume of a pyramid. In order to compare theoretical with experimental techniques, the above sections were tested and the value $\frac{T}{k}$ determined. The average per cent deviation from theory was 5.05 per cent.

Circular Section

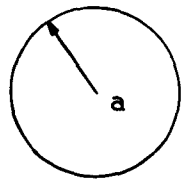


a = 5 inches

Theory[24] $\quad \frac{T}{k} = \frac{2\pi a^3}{3} = \frac{2\pi(125)}{3} = 261.5$

Experiment $\quad \frac{T}{k} = \frac{2V}{m}$, V = 82.8 cubic inches (determined by weighing)

m = 0.636 (determined by measuring microscope)

$\frac{T}{k} = \frac{(2)(82.8)}{0.636} = 260.5$. Therefore, per cent deviation from theory is 0.384%.

Square Section

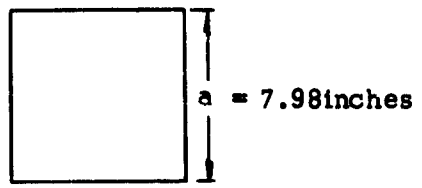


Theory $\frac{T}{k} = \frac{a^3}{3} = \frac{(7.98)^3}{3} = 169.7$

Experiment $\frac{T}{k} = \frac{2V}{m}$

V = 57.5 cubic inches

$$\frac{T}{k} = \frac{(2)(57.5)}{0.636} = 181$$

Per cent deviation from theory is 6.67%.

Rectangular Section

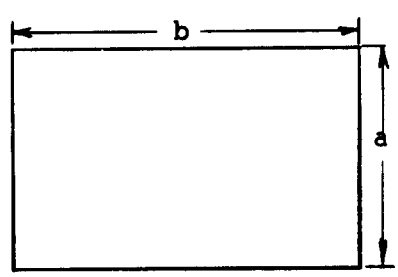


a = 6.06 inches
b = 8.03 inches

Theory $\frac{T}{k} = \frac{a^3}{3} + \frac{a^2(b-a)}{2}$

$$\frac{T}{k} = \frac{(6.06)^3}{3} + \frac{(606)^2[8.03-6.06]}{2} = 100.5$$

Experiment $\frac{T}{k} = \frac{2}{m}V = \frac{2}{0.636}(34.7) = 109$

Per cent deviation from theory is 8.1%.

## LITERATURE CITED


1. G. Murphy, Advanced Mechanics of Materials (McGraw-Hill Book Company, Inc., New York, 1946), p. 48.

2. Ibid.

3. S. Timoshenko and J. N. Goodier, Theory of Elasticity (McGraw-Hill Book Company, Inc., New York, 1951), p. 259.

4. Ibid., p. 260.

5. Ibid., p. 261.

6. J. P. Den Hartog, Advanced Strength of Materials (McGraw-Hill Book Company, Inc., New York, 1952), p. 1.

7. Timoshenko, op. cit., p. 229.

8. A. Nadai, Theory of Flow and Fracture of Solids (McGraw-Hill Book Company, Inc., New York, 1950), p. 493.

9. Murphy, op. cit., p. 159.

10. Ibid., p. 161.

11. A. A. Griffith and G. I. Taylor, Tech. Dept. Nat'l Advisory Comm. Aeronaut., vol. 3, p. 938 (1918).

12. M. Hetenyi, Handbook of Experimental Stress Analysis (John Wiley and Sons, New York, 1950), pp. 723-726.

13. W. Prager and P. J. Hodge, Jr., Theory of Perfectly Plastic Solids (John Wiley and Sons, Inc., New York, 1951), p. 22.

14. Ibid., p. 34.

15. Ibid., p. 24.

16. Nadai, op. cit., p. 209.

17. Ibid., p. 494.

18. M. A. Sadowsky, "An Extension of the Sand-Heap Analogy in Plastic Torsion Applicable to Cross Sections Having One or More Holes," Journ. of Applied Mechanics, December 1941.

19. Murphy, op. cit., p. 186.

20. Sadowsky, op. cit., p. 166.

21. G. Murphy, Similitude in Engineering (Ronald Press Company, New York, 1950), p. 36.

22. A. Phillips, Introduction to Plasticity (Ronald Press Company, New York, 1956), p. 7.

23. Nadai, op. cit., p. 490.

24. Ibid., p. 498.

## BIBLIOGRAPHY


Den Hartog, J. P., Advanced Strength of Materials. New York: McGraw-Hill Book Company, 1952.

Durelli, A. J., et al., Introduction to the Theoretical and Experimental Analysis of Stress and Strain. New York: McGraw-Hill Book Company, 1958.

Griffith, A. A., and G. I. Taylor, Technical Report National Advisory Committee for Aeronautics, vol. 3, 1917-1918. Washington: Government Printing Office.

Hetenyi, M., Handbook of Experimental Sttess Analysis. New York: John Wiley and Sons, 1950.

Marin, J., Mechanical Behavior of Engineering Materials. Englewood Cliffs, New Jersey: Prentice Hall, 1962.

Murphy, G., Advanced Mechanics of Materials. New York: McGraw-Hill Book Company, 1946.

_____, Similitude in Engineering. New York: Ronald Press Company, 1950.

Nadai, A., Plasticity. Engineering Society Monograph, New York: McGraw-Hill Book Company, 1931.

_____, Theory of Flow and Fracture of Solids. New York: McGraw-Hill Book Company, 1950.

Phillips, A., Introduction to Plasticity. New York: Ronald Press Company, 1956.

Prager, W., and P. G. Hodge, Jr., Theory of Perfectly Plastic Solids. New York: John Wiley and Sons, 1951.

Sadowsky, M. A., "An Extension of the Sand-Heap Analogy in Plastic Torsion Applicable to Cross Sections Having One or More Holes," Journal of Applied Mechanics, December 1941, Vol. 8, No. 4, p. A-166.

Timoshenko, S., and J. N. Goodier, Theory of Elasticity. New York: McGraw-Hill Book Company, 1951.

Trayer, G. W., and H. W. March, "The Torsion of Members Having Sections Common in Aircraft Construction," NACA Report No. 334, Washington: U. S. Government Printing Office.

Westergaard, H. M., Theory of Elasticity and Plasticity. Cambridge: Harvard University Press, 1952.

_____, "Graphostatics of Stress Functions," Transactions of the American Society of Mechanical Engineers, March 1934, Vol. 56, No. 3, p. 141.